tvst

Article

Influence of Lens Fluorescence on Fluorescence Lifetime Imaging Ophthalmoscopy (FLIO) Fundus Imaging and Strategies for Its Compensation

Jakob Lauritz Brauer[1], Rowena Schultz[1], Matthias Klemm[2], and Martin Hammer[1,3]

[1] Department of Ophthalmology, University Hospital Jena, Jena, Germany
[2] Technical University Ilmenau, Institute for Biomedical Techniques and Informatics, Ilmenau, Germany
[3] Center for Medical Optics and Photonics, University of Jena, Jena, Germany

Correspondence: Martin Hammer, Department of Ophthalmology, University Hospital Jena, Am Klinikum 1, 07747 Jena, Germany. e-mail: martin.hammer@med.uni-jena.de

Received: December 20, 2019
Accepted: April 15, 2020
Published: July 9, 2020

Keywords: fundus autofluorescence; fluorescence lifetime; lens fluorescence; cataract

Citation: Brauer JL, Schultz R, Klemm M, Hammer M. Influence of lens fluorescence on fluorescence lifetime imaging ophthalmoscopy (FLIO) fundus imaging and strategies for its compensation. Trans Vis Sci Tech. 2020;9(8):13, https://doi.org/10.1167/tvst.9.8.13

Purpose: To explore the contribution of crystalline lens fluorescence to fluorescence lifetimes measured with fluorescence lifetime imaging ophthalmoscopy (FLIO) and to propose a computational model to reduce the lens influence.

Methods: FLIO, which detects autofluorescence decay over time in a short-wavelength spectral channel (SSC, 498–560 nm) and a long-wavelength spectral channel (LSC, 560–720 nm), was performed on 32 patients before and after cataract extraction. The mean autofluorescence lifetime (τ_m) of the fundus was determined from a three-exponential fit of the postoperative fluorescence decays. The preoperative measurements were fit with series of exponential functions in which one fluorescence component was time-shifted in order to represent lens fluorescence.

Results: Postoperatively, τ_m was 185 $\pm$ 22 ps in the SSC and 209 $\pm$ 34 ps in the LSC at the posterior pole. These values were best reproduced by fitting the postoperative measurements with a three-exponential model with a time-shifted third fluorescence component (SSC, 203 $\pm$ 45 ps; LSC, 215 $\pm$ 29 ps), whereas disregarding time-shifted lens fluorescence resulted in significantly ($P < 0.001$) longer τ_m values (SSC, 474 $\pm$ 206 ps; LSC, 215 $\pm$ 29 ps). The fluorescence of the cataract lens contributed to the total fluorescence by 54.2 $\pm$ 10.6% (SSC) and 29.5 $\pm$ 9.9% (LSC).

Conclusions: Cataract lens fluorescence greatly alters fluorescence lifetimes measured at the fundus by FLIO, resulting in an overestimation of the lifetimes; however, this may be compensated for considerably by taking lens influence into account in the fitting model.

Translational Relevance: This study investigates cataract fluorescence in FLIO and a mathematical model for compensation of this influence.

Introduction

Fluorescence lifetime imaging ophthalmoscopy (FLIO) is a novel imaging modality that allows for molecular in vivo imaging of the retina and retinal pigment epithelium. FLIO may be able to distinguish different fluorophores or alteration of their environment by their fluorescence lifetime.[1–3] The technique is used in experimental diagnostic trials for various retinal diseases,[4–18] as well as in animal studies.[19,20] Its reproducibility has been validated in three studies, where the coefficient of variation was found to be below 20%.[13,21,22] The technique is based on confocal scanning laser ophthalmoscopy, which greatly eliminates fluorescence light from the lens. However, the lens of the human eye shows extraordinarily strong fluorescence, especially in the case of cataract (Fig. 1), which arises from tryptophan as well as non-tryptophan peptides.[23] Lens fluorescence increases with age[24,25] and, especially, with cataract[23] or diabetes.[26] With aging, post-translational protein changes take place; for example, tryptophan oxidation results in aromatic products with absorption and emission in the visible

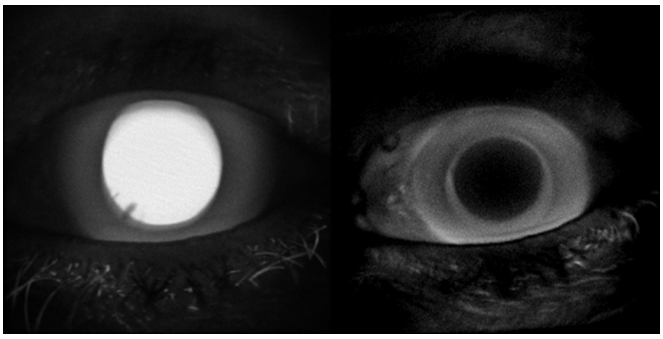

Figure 1. Fluorescence intensity image of the anterior part of the eye of a 68-year-old patient before (*left*) and after (*right*) cataract extraction.

spectral range.[23] Non-tryptophan fluorescence has been attributed to the insoluble protein fraction.[27] In the aging lens, peptide fluorescence increases due to the formation of 3-hydroxykynurenine glucoside,[28] 4-(2-amino-3-hydroxyphenyl)-4-oxobutanoic acid,[29] and glutathione-3-hydroxykynurenine glycoside.[30] Thus, fluorescence measurements at the retina are likely influenced by a superimposition of the lens fluorescence. Because the fluorescence lifetime of the lens is longer than that measured from the retina and retinal pigment epithelium,[1] increased mean lifetimes in FLIO readings in elderly patients[13] might be skewed by lens fluorescence. For this reason, Klemm et al.[31] introduced a layered components model for fitting fluorescence decays that makes use of the fact that the lens is anterior to the fundus, so fluorescence light from the lens will arrive at the detector earlier. Ideally, this should separate fluorescence components from the fundus and from the lens; however, this approach was never tested in a patient population. Thus, in this study, we analyzed FLIO readings of patients who underwent cataract surgery. As the fluorescence of the artificial intraocular lens can be assumed to be negligible (Fig. 1), the lifetimes of the postoperative measurements were assumed to be those of the fundus. This study aimed to understand changes in fluorescence lifetimes in cataracts. Measurements were done pre- and postoperatively, and various mathematical models were applied to identify a model that minimizes influence of the lens.

Methods

Patients

Thirty-two patients (mean age, 72.3 years; SD, 9.3 years; range, 49–88 years) scheduled for cataract extraction were included in this study. Sixteen patients were female, and 16 were male. The study followed the tenets of the Declaration of Helsinki and was approved by a local ethics committee. Informed consent was obtained from all subjects before inclusion. All patients were diagnosed with cataracta provecta, and no distinction between nuclear or cortical cataract was made. Patients suffering from ophthalmic diseases other than cataract or from systemic diseases known to influence ocular fundus autofluorescence[3] were excluded. Specifically, we excluded patients with age-related macular degeneration, cardiovascular disease (except well-controlled hypertension), macular telangiectasia, retinitis pigmentosa, retina vascular occlusions, hereditary retinal diseases such as Stargardt disease and choroideremia, central serous chorioretinopathy, Alzheimer's disease, or albinism. All investigations were performed 1 day before and on average 33.2 (± 10.3) days after cataract extraction.

Procedures

All patients received a full ophthalmic investigation, including slit-lamp biomicroscopy, funduscopy, and measurement of intraocular pressure. The pupils were dilated using tropicamid (Mydriaticum Stulln, Pharma Stulln GmbH, Nabburg, Germany) and phenylephrin-hydrochloride (Neosynephrin-POS 5%, Ursapharm GmbH, Saarbrucken, Germany). The patients then received FLIO imaging. In addition to the fundus FLIO, a recording of the fluorescence of the lens was taken. In order to standardize this measurement, the device was set at the maximum possible distance from the patient and focused onto the anterior part of the eye. At least 1000 photons per pixel were recorded, and the lifetimes were determined from a standardized square in the center of the lens. No sodium fluorescein was administered to the cornea or by intravenous injection prior to FLIO investigation. The basic principles and laser safety precautions for FLIO are described elsewhere.[9,13,32] Briefly, a picosecond laser diode was coupled to a laser scanning ophthalmoscope (Spectralis; Heidelberg Engineering, Heidelberg, Germany) for autofluorescence excitation at 473 nm with a repetition rate of 80 MHz. Fluorescence photons were detected by time-correlated, single-photon counting (SPC-150 TCSPC Module; Becker & Hickl GmbH, Berlin, Germany) in a short-wavelength spectral channel (SSC, 498–560 nm) and a long-wavelength spectral channel (LSC, 560–720 nm). FLIO provides 30° images with a frame rate of 9 frames per second and a resolution of 256 × 256 pixels.

Models for the Approximation of Fluorescence Decays

For the approximation of lifetimes, we used FLIMX software,[31] which is documented and freely available for download online under the open-source BSD license (http://www.flimx.de). Photon histograms over time, describing the autofluorescence decay, were least square fitted with a series of three exponential functions:

$$I(t) = IRF * \sum_{i=1}^{3} a_i \cdot e^{-\frac{t}{\tau_i}} \quad (1)$$

where $I(t)$ is the fluorescence intensity at time t, IRF is the instrument response function of the device, I_0 is the intensity at $t = 0$, τ_i are the time constants of fluorescence decay, a_i describe their abundance, and the asterisk denotes a convolution integral. This three-exponential fit of fluorescence decay is widely used in FLIO and is here denoted as model 0. The amplitude-weighted mean decay time (τ_m) was used for further analysis, and the τ_m of the postoperative measurements is considered the mean lifetime of the fundus. The relative contribution of each fluorescence component was defined by

$$Q_i = \frac{a_i \cdot \tau_i}{\sum_i a_i \cdot \tau_i} \quad (2)$$

For the fit of the preoperative measurements, four different models, taking lens fluorescence into account, were investigated. Model 1:

$$I(t) = IRF * \left(a_1 \cdot e^{-\frac{t}{\tau_1}} + a_2 \cdot e^{-\frac{t}{\tau_2}} + a_3 \cdot e^{-\frac{t-150ps}{\tau_3}}\right) \quad (3)$$

was adopted from the suggestions of the SPC-150 TCSPC Module manufacturer, Becker & Hickl GmbH,[33] and assumes two fluorescence components from the fundus, represented by the lifetimes τ_1 and τ_2, and one component from the lens (τ_3), which is shifted against the fundus fluorescence by –150 ps. This is roughly the time it takes the light to travel the vitreous twice. Consequently, in this model, τ_m is calculated from τ_1 and τ_2, weighted by a_1 and a_2 only. In order to be consistent with the postoperative analysis when using three lifetime components at the fundus, we also established and tested four-exponential models. Model 2:

$$I(t) = IRF * \left(a_1 \cdot e^{-\frac{t}{\tau_1}} + a_2 \cdot e^{-\frac{t}{\tau_2}} + a_3 \cdot e^{-\frac{t}{\tau_3}} + a_4 \cdot e^{-\frac{t-150ps}{\tau_4}}\right) \quad (4)$$

assumes three components, τ_1, τ_2, and τ_3, from which τ_m is calculated, representing the fundus fluorescence, whereas the time-shifted τ_4 represents the lens fluorescence. We do not know whether the lifetime of the lens or the slowest decay component from the fundus is larger; however, the software assumes $\tau_1 < \tau_2 < \tau_3 < \tau_4$. Therefore, model 3:

$$I(t) = IRF * \left(a_1 \cdot e^{-\frac{t}{\tau_1}} + a_2 \cdot e^{-\frac{t}{\tau_2}} + a_3 \cdot e^{-\frac{t-150ps}{\tau_3}} + a_4 \cdot e^{-\frac{t}{\tau_4}}\right) \quad (5)$$

was tested, where τ_3 represents the time-shifted lens fluorescence and τ_4 a very slow fundus fluorescence. Finally, we used the mean lifetime measured from the lens, instead of a free fitting parameter, as τ_3 in Equation 5, denoted as model 4. In models 3 and 4, τ_m was calculated from τ_1, τ_2, and τ_4 and the respective amplitudes. Fixating τ_4 in Equation 4 to the lens lifetime resulted in poor fits (data not shown). Thus, this approach was not pursued further.

For all approximations, τ_m was averaged over the central area, the inner and outer ring, and the whole field of the standardized Early Treatment Diabetic Retinopathy Study (ETDRS) grid. These values were compared for all fits (models 0 through 4) of the preoperative measurements with those of the postoperative measurements (model 0) in paired t-tests using SPSS Statistics 26 (IBM, Armonk, NY, USA). Furthermore, Spearman correlation coefficients were determined. In order to obtain an estimate of the relative contribution of lens fluorescence to total fluorescence, the Q value of the shifted fluorescence component was calculated. This is the product of the respective a and τ values (e.g., a_3 and τ_3 for model 1, a_4 and τ_4 for model 2) normalized to the total fluorescence.

Results

One patient had to be excluded because the cataract was too dense to obtain a preoperative FLIO measurement of the fundus. Figure 2 shows an example of color-coded τ_m from the postoperative measurement, as well as models 0 through 4 applied to the preoperative measurement in both spectral channels. Because the color-coding is the same for all panels per channel, this figure clearly demonstrates the overestimation of the fluorescence lifetime due to including all fluorescence components in the calculation of τ_m (compare postoperative and model 0 panels). This particularly holds true for the SSC. In contrast, models 1 and 2 showed fit results similar to the postoperative results, although those of model 2 are noisier. The lifetimes, given by models 3 and 4, are considerably longer than the postoperatively measured lifetimes. Despite these differences in the results, all models were able to fit the measured decays well. Supplementary

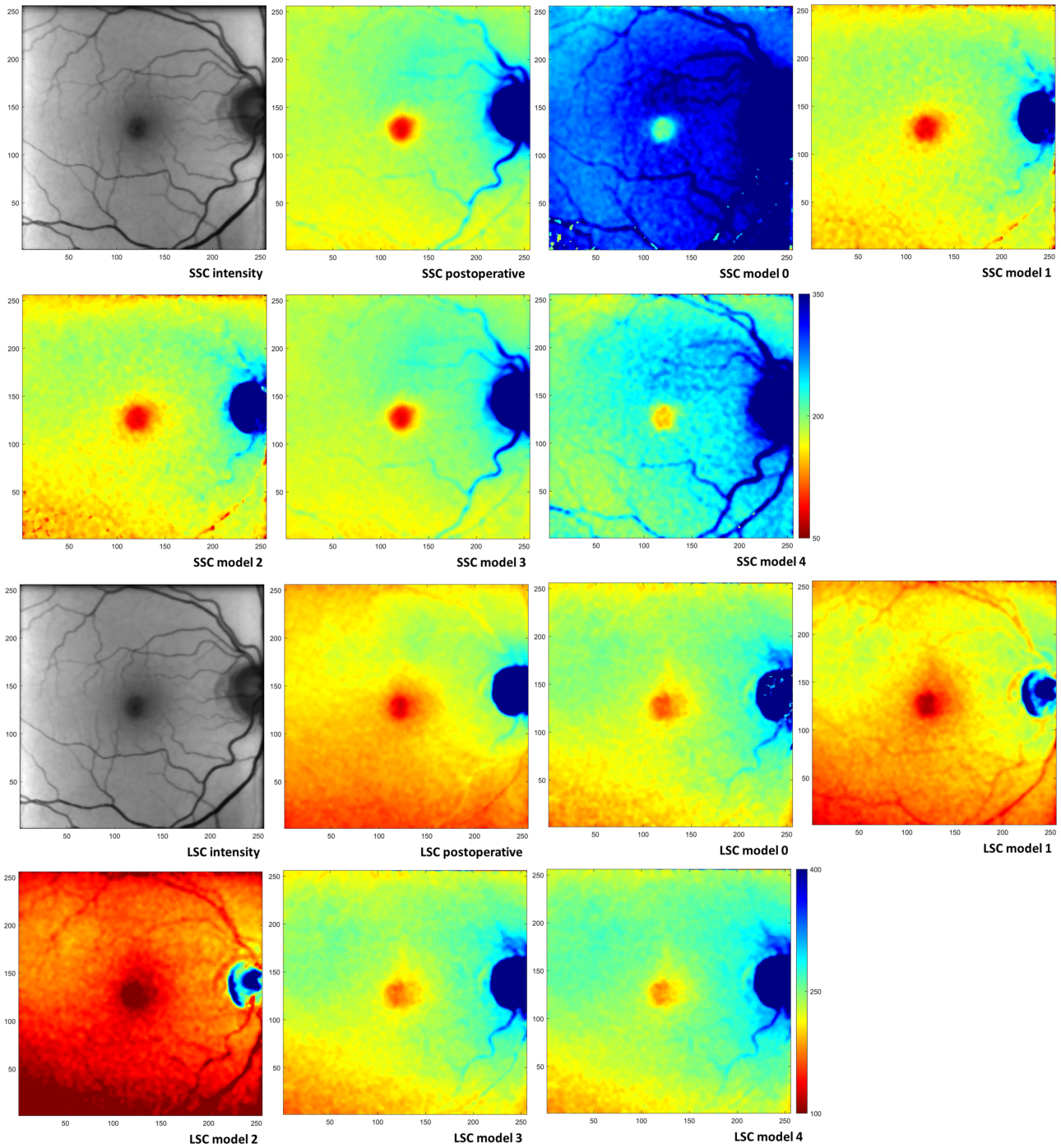

Figure 2. FLIO images of a 71-year-old subject. (*Top row, left to right*) SSC: fluorescence intensity postoperative, mean lifetime τ_m postoperative, τ_m preoperative model 0, and τ_m preoperative model 1. (*Second row, left to right*) SSC: τ_m preoperative model 2, τ_m preoperative model 3, and τ_m preoperative model 4. Color-coding of lifetimes is identical (50–350 ps) for all panels in the first two rows. (*Third row, left to right*) LSC: fluorescence intensity postoperative, τ_m postoperative, τ_m preoperative model 0, and τ_m preoperative model 1. (*Bottom row, left to right*) LSC: τ_m preoperative model 2, τ_m preoperative model 3, and τ_m preoperative model 4. Color-coding of lifetimes is identical (50–400 ps) for all panels in the last two rows. Images are scaled in pixels; the size of 1 pixel is 35 $\times$ 35 μm^2 in an emmetropic eye. The preoperative fluorescence intensity image in SSC is shown in Supplementary Figure S1.

Table 1. Mean Values (SD) Over All Subjects for Mean Lifetime τ_m (ps)*

	Center Circle	*P*	Inner Ring	*P*	Outer Ring	*P*	Full Circle	*P*
SSC								
Postoperative	109 (25)		171 (23)		192 (24)		185 (22)	
Model 0	491 (195)	<0.001	480 (224)	<0.001	474 (200)	<0.001	474 (206)	<0.001
Model 1	135 (44)	<0.001	189 (45)	0.014	210 (46)	0.02	203 (45)	0.017
Model 2	134 (47)	0.001	187 (50)	0.046	209 (51)	0.043	202 (50)	0.04
Model 3	297 (184)	<0.001	351 (189)	<0.001	344 (160)	<0.001	344 (167)	<0.001
Model 4	287 (147)	<0.001	339 (145)	<0.001	344 (129)	<0.001	341 (133)	<0.001
LSC								
Postoperative	146(30)		196 (33)		216 (35)		209 (34)	
Model 0	266(97)	<0.001	293 (75)	<0.001	300 (67)	<0.001	298 (69)	<0.001
Model 1	151(33)	0.285	202 (29)	0.183	222 (30)	0.175	215 (29)	0.175
Model 2	117(37)	<0.001	161 (47)	<0.001	182 (51)	<0.001	175 (49)	<0.001
Model 3	227(78)	<0.001	243 (68)	0.001	247 (64)	0.019	245 (64)	0.007
Model 4	212(50)	<0.001	246 (53)	<0.001	255 (54)	<0.001	252 (53)	<0.001

*From the postoperative three-exponential fit (model 0) and preoperative fits according to models 0 to 4, as well as *P* values for the paired *t*-tests of the pre- versus postoperative fits in the center, inner, and outer ring and full circle of the ETDRS grid. Bonferroni correction for multiple testing was applied to the *P* values.

Figure S2 shows the decay curve along with model fit for a 100 × 100 pixel from one patient; the residuals of the fit are plotted at the bottom of each panel.

The mean values of τ_m over all 31 patients are shown in Table 1 for the postoperative FLIO measurements (model 0), as well as for the preoperative measurements (models 0 through 4; see Supplementary Tables S1 and S2 for single lifetime components τ_1 through τ_4 and their relative amplitudes, a_1 through a_4). *P* values for the paired comparisons of the postoperative data with the respective model fits of the preoperative measurements are also given. In all regions of the ETDRS grid, the three-exponential fit (model 0) resulted in considerably longer τ_m values for the preoperative measurements than for the postoperative ones. Also, τ_m values for models 3 and 4, assuming a shifted third fluorescence component from the lens, greatly deviate from the postoperative results (Table 1). Thus, in the following, we focus on models 1 and 2, applying lens fluorescence to the longest living decay component. The application of these models is shown in Figure 3 for three more cases.

The relative contributions of the third (Q_3 in model 1) and fourth (Q_4 in model 2) fluorescence components consistently indicated a considerable amount of total fluorescence: Q_3 values were 54.2 ± 10.6% (SSC) and 29.5 ± 9.9% (LSC), and Q_4 values were 52.6 ± 11.1% (SSC) and 25.2 ± 11.2% (LSC), all measured in the full circle of the ETDRS grid. Mean lifetimes of the lens, measured from FLIO images of the anterior part of the eye, were 2813 ± 349 ps (SSC) and 1951 ± 252 ps (LSC).

Furthermore, we explored the correlations between pre- and postoperative τ_m (Table 2). These are shown in Figure 4 for the full circle of the ETDRS grid. The figure also shows only minor differences between model 1 and model 2. The differences between postoperative measurements and models 1 and 2 for preoperative measurements are shown in Bland–Altman plots (Fig. 4). The absolute values of the differences for the full circle were 32 and 36 ps (SSC, models 1 and 2) and 20 and 42 ps (LSC, models 1 and 2), on average. These values were smaller than the respective standard deviations of the inter-individual variances: 45 and 50 ps (SSC, models 1 and 2) and 29 and 49 ps (LSC, models 1 and 2).

Discussion

Lens fluorescence considerably influences fluorescence lifetimes measured at the retina by FLIO. This is reflected by the more than 2.5-times longer lifetimes (SSC full circle; see Table 1 and Fig. 2) for model 0 compared to the postoperative measurements. As the same fit models were used, this difference has to be attributed to the lens. Even in non-cataract eyes, lens fluorescence seems to influence the fundus FLIO readings in an age-dependent manner. Dysli et al.[13] showed an increase of τ_m with age in healthy subjects. Because this increase was larger for the non-dilated

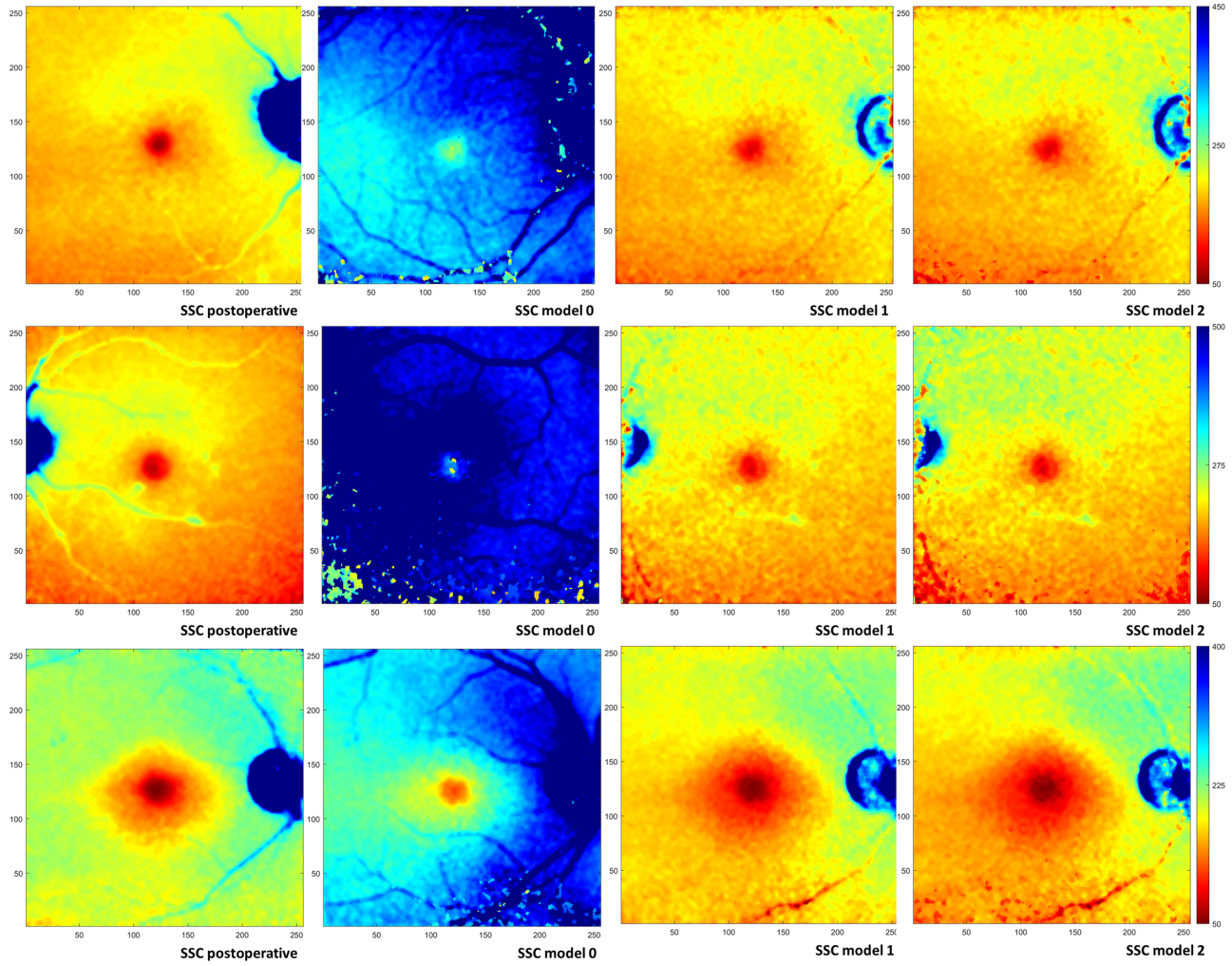

Figure 3. FLIO images (SSC) of subjects who were 74 years old (*top row*), 77 years old (*middle row*), and 80 years old (*bottom row*). (*Left to right*) Mean lifetime τ_m postoperative, τ_m preoperative model 0, τ_m preoperative model 1, and τ_m preoperative model 2. Color-coding is scaled identically for all models per subject as indicated (50–450 ps, 50–500 ps, and 50–400 ps, respectively). Images are scaled in pixels; the size of 1 pixel is 35 × 35 µm^2 in an emmetropic eye.

than for the dilated pupil, these authors argued that the age dependence of the lifetimes, at least partially, could result from lens fluorescence. Here, we were able to quantify the influence of the cataract lens to fundus FLIO measurements. Fitting the preoperative measurements with the three-exponential decay model (model 0), which is used in most publications, resulted in an overestimation of the lifetimes (τ_m) by 320 ps (173%) in the SSC and by 100 ps (48%) in the LSC, as is apparent from the comparison with postoperative measurements in the full ETDRS grid. For the macula, this overestimation is even higher (Table 1). This overestimation clearly results from the fluorescence of the cataract lens, which contributed to the total measured fluorescence by 5% to 55% in the SSC and by 25% to 30% in the LSC, as indicated by Q_3 and Q_4 in models 1 and 2, respectively. This raises an urgent need to compensate for lens fluorescence. This could be achieved by changing the optical setup by introducing an aperture diaphragm separation, as suggested by Klemm et al.[34] Because such a change has not been implemented in the FLIO device, we relied on the temporal anteriority of the lens fluorescence compared to that of the fundus. This can be observed as a step-shaped distortion of the rising edge of the fluorescence.[31] Because the width of the instrument response function of the FLIO device is on the order of the time difference between lens and fundus fluorescence, this step is difficult to detect in conventional FLIO but was more clearly demonstrated by Becker et al.[33] using an ultra-fast detector. However, the time shift of lens fluorescence can also be derived from data obtained with the FLIO device currently used in clinical investigations.[31] Accordingly, this approach was

Table 2. Pearson Correlation Coefficients (R^2) and Respective *P* Values Describing the Association of Postoperative τ_m with Preoperative Fits According to Models 1 and 2 in the Center, Inner, and Outer Ring and Full Circle of the ETDRS Grid

	Center Circle	*P*	Inner Ring	*P*	Outer Ring	*P*	Full Circle	*P*
SSC								
Model 1	0.339	<0.001	0.320	<0.001	0.187	0.015	0.203	0.011
Model 2	0.324	<0.001	0.320	<0.001	0.176	0.019	0.201	0.012
LSC								
Model 1	0.507	<0.001	0.471	<0.001	0.561	<0.001	0.528	<0.001
Model 2	0.258	0.04	0.208	0.01	0.202	0.011	0.198	0.012

tested by Becker et al.[33] on one subject using a three-exponential model with one shifted component (model 1). We expanded this approach to more decay models and tested them in a cohort of 31 patients, large enough to obtain statistically reliable results.

Models 3 and 4 failed, as they were not able to reproduce the postoperative mean fluorescence lifetimes assumed to be the ground truth of ocular fundus fluorescence. Model 1 resulted in mean values of τ_m that were closest to those of the postoperative measurements for all fields of the ETDRS grid (Table 1). Furthermore, τ_m values from model 1 showed the highest correlation coefficients with the postoperative τ_m values (Table 2). Agreement between model 1 and the postoperative measurements was better for the LSC than for the SSC. This is reasonable, because the lens emits fluorescence in the blue and green spectral range.[23,30] Thus, the LSC (above 560 nm) is less disturbed by lens fluorescence. This is further supported by the fact that the deviation of model 0 from the postoperative data is much more pronounced in the SSC than in the LSC. However, it must be noted that the correlation between the results from model 1 and the postoperative measurements is weak (SSC, $R^2 = 0.203$; LSC, $R^2 = 0.528$) (Fig. 4). This means that the compensation for lens fluorescence by model 1 did not work equally well in all patients. Nevertheless, deviations of the pre- and postoperative measurements are much lower with the correction (model 1) than without (model 0). The correction in model 1 resulted in τ_m values for which differences from postoperative measures were below the standard deviations of the inter-individual variances (Fig. 4, Bland–Altman plots).

Model 2 worked as well as model 1 for the SSC (see data in Tables 1 and 2) but was inferior for the LSC. From a theoretical point of view, however, model 2 should be favored. Consistent with the fits of the postoperative measurements, model 2 assumes three decay components for the fundus fluorescence, and the non-zero a_3, found in pseudophakic eyes, indicates that there is a slow-decaying fluorescence component from the fundus. One reason for the potential superiority of model 1 might be the higher numerical stability of fit, as it uses six free parameters and model 2 has to determine eight parameters (Equations 3 and 4). Also, the τ_m values for models 1 and 2 were strongly correlated (for the full circle, $R^2 = 0.98$ for the SSC and $R^2 = 0.92$ for the LSC), so model 1 can be assumed to give a good estimate of the fundus fluorescence lifetimes in cataract eyes.

Just by its design, this study has some limitations. The main limitation is its restriction to cataract patients. This was necessary in order to utilize postoperative reference values; with the current optics of the FLIO device, it is impossible to measure the fundus fluorescence without perturbation of that of the lens in phakic eyes. This, however, restricts the preference for model 1, supported by our data, to cataract eyes. We cannot say whether this also holds true for non-cataract eyes or if another model would be more appropriate. Furthermore, although the fit according to model 1 works very well on average, deviations in single subjects were remarkable. In this study, we did not differentiate among the various kinds and severity levels of cataracts, as our study population was too small for the investigation of subgroups. Thus, we cannot tell whether abovementioned deviations are related to cataract type or severity.

In conclusion, we were able to show that lens fluorescence contributes considerably to the FLIO signal and greatly alters the measured fundus fluorescence lifetimes. However, a mean fluorescence lifetime (τ_m), calculated as the amplitude-weighted average of τ_1 and τ_2 from a three-exponential fit of the measurements in which τ_3 was temporally shifted and assumed to represent lens fluorescence (model 1), was close to the fundus lifetime measured in the same eyes after cataract extraction, on average. Future experiments should investigate factors influencing individual

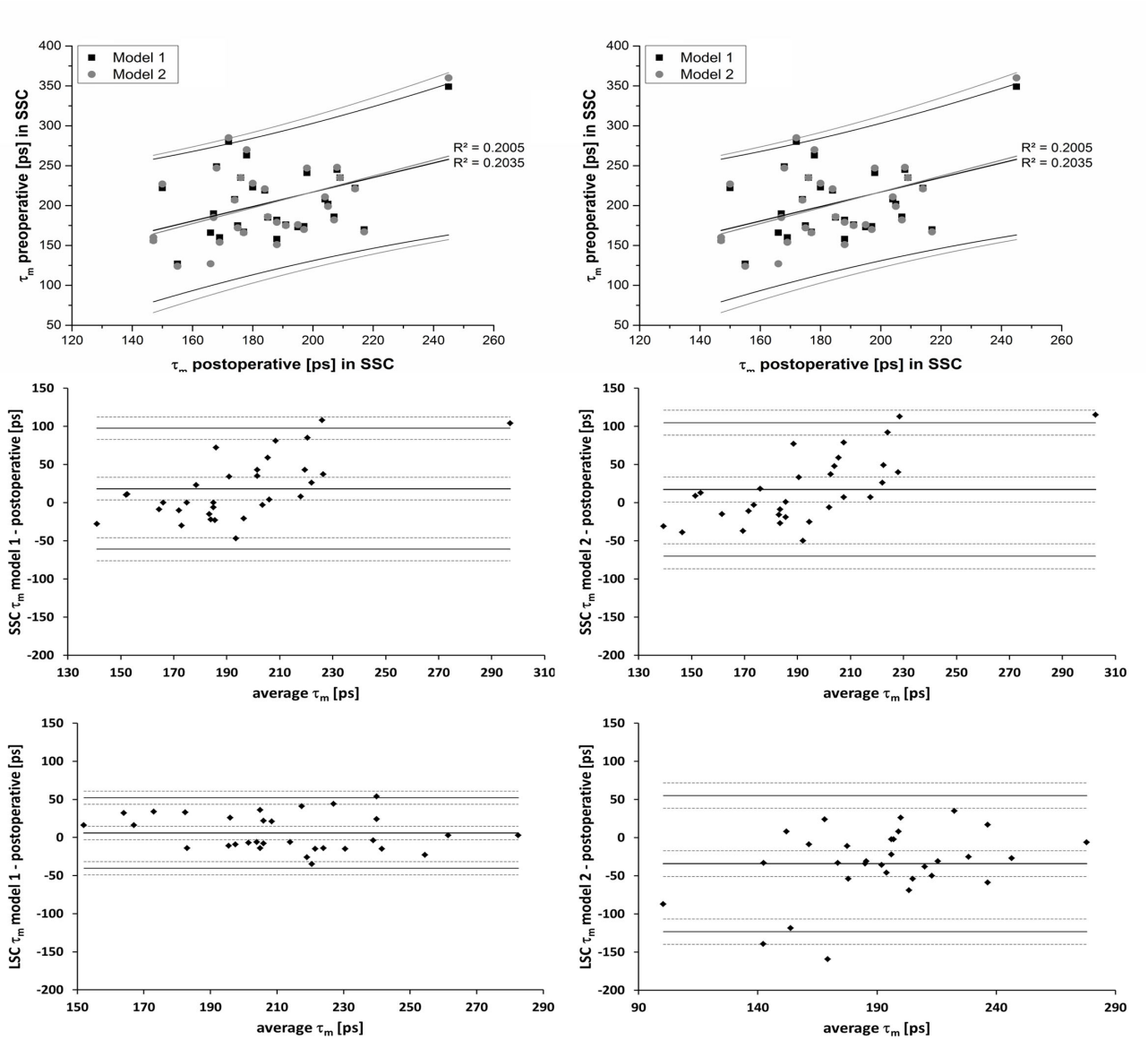

Figure 4. Correlation between postoperative and preoperative (models 1 and 2) mean lifetimes (τ_m) in the SSC (*top left*) and LSC (*top right*) for the full circle of the ETDRS grid along with Bland–Altman plots of the differences of τ_m between both preoperative models and the postoperative measurement for the SSC (*middle*) and LSC (*bottom*). Dashed lines indicate 95% confidence intervals for the limits of agreement.

cataract effects, as well as the applicability of this model to eyes without cataract.

Acknowledgments

Disclosure: **J.L. Brauer,** None; **R. Schultz,** None; **M. Klemm,** None; **M. Hammer**, P

References

1. Schweitzer D, Schenke S, Hammer M, et al. Towards metabolic mapping of the human retina. *Microsc Res Tech*. 2007;70:410–419.
2. Dysli C, Wolf S, Berezin MY, Sauer L, Hammer M, Zinkernagel MS. Fluorescence lifetime imaging ophthalmoscopy. *Prog Retin Eye Res*. 2017;60:120–143.

3. Sauer L, Andersen KM, Dysli C, Zinkernagel MS, Bernstein PS, Hammer M. Review of clinical approaches in fluorescence lifetime imaging ophthalmoscopy. *J Biomed Opt*. 2018;23:1–20.
4. Sauer L, Andersen KM, Li B, Gensure RH, Hammer M, Bernstein PS. Fluorescence lifetime imaging ophthalmoscopy (FLIO) of macular pigment. *Invest Ophthalmol Vis Sci*. 2018;59:3094–3103.
5. Sauer L, Gensure RH, Andersen KM, et al. Patterns of fundus autofluorescence lifetimes in eyes of individuals with nonexudative age-related macular degeneration. *Invest Ophthalmol Vis Sci*. 2018;59:AMD65–AMD77.
6. Sauer L, Gensure RH, Hammer M, Bernstein PS. Fluorescence lifetime imaging ophthalmoscopy: a novel way to assess macular telangiectasia type 2. *Ophthalmol Retina*. 2018;2:587–598.
7. Sauer L, Klemm M, Peters S, et al. Monitoring foveal sparing in geographic atrophy with fluorescence lifetime imaging ophthalmoscopy – a novel approach. *Acta Ophthalmol*. 2018;96:257–266.
8. Sauer L, Peters S, Schmidt J, et al. Monitoring macular pigment changes in macular holes using fluorescence lifetime imaging ophthalmoscopy. *Acta Ophthalmol*. 2017;95:481–492.
9. Sauer L, Schweitzer D, Ramm L, Augsten R, Hammer M, Peters S. Impact of macular pigment on fundus autofluorescence lifetimes. *Invest Ophthalmol Vis Sci*. 2015;56:4668–4679.
10. Schmidt J, Peters S, Sauer L, et al. Fundus autofluorescence lifetimes are increased in nonproliferative diabetic retinopathy. *Acta Ophthalmol*. 2017;95:33–40.
11. Dysli C, Berger L, Wolf S, Zinkernagel MS. Fundus autofluorescence lifetimes and central serous chorioretinopathy. *Retina*. 2017;37:2151–2161.
12. Dysli C, Fink R, Wolf S, Zinkernagel MS. Fluorescence lifetimes of drusen in age-related macular degeneration. *Invest Ophthalmol Vis Sci*. 2017;58:4856–4862.
13. Dysli C, Quellec G, Abegg M, et al. Quantitative analysis of fluorescence lifetime measurements of the macula using the fluorescence lifetime imaging ophthalmoscope in healthy subjects. *Invest Ophthalmol Vis Sci*. 2014;55:2106–2113.
14. Dysli C, Schurch K, Pascal E, Wolf S, Zinkernagel MS. Fundus autofluorescence lifetime patterns in retinitis pigmentosa. *Invest Ophthalmol Vis Sci*. 2018;59:1769–1778.
15. Dysli C, Wolf S, Hatz K, Zinkernagel MS. Fluorescence lifetime imaging in Stargardt disease: potential marker for disease progression. *Invest Ophthalmol Vis Sci*. 2016;57:832–841.
16. Dysli C, Wolf S, Tran HV, Zinkernagel MS. Autofluorescence lifetimes in patients with choroideremia identify photoreceptors in areas with retinal pigment epithelium atrophy. *Invest Ophthalmol Vis Sci*. 2016;57:6714–6721.
17. Dysli C, Wolf S, Zinkernagel MS. Fluorescence lifetime imaging in retinal artery occlusion. *Invest Ophthalmol Vis Sci*. 2015;56:3329–3336.
18. Dysli C, Wolf S, Zinkernagel MS. Autofluorescence lifetimes in geographic atrophy in patients with age-related macular degeneration. *Invest Ophthalmol Vis Sci*. 2016;57:2479–2487.
19. Dysli C, Dysli M, Enzmann V, Wolf S, Zinkernagel MS. Fluorescence lifetime imaging of the ocular fundus in mice. *Invest Ophthalmol Vis Sci*. 2014;55:7206–7215.
20. Dysli C, Dysli M, Zinkernagel MS, Enzmann V. Effect of pharmacologically induced retinal degeneration on retinal autofluorescence lifetimes in mice. *Exp Eye Res*. 2016;153:178–185.
21. Klemm M, Dietzel A, Haueisen J, Nagel E, Hammer M, Schweitzer D. Repeatability of autofluorescence lifetime imaging at the human fundus in healthy volunteers. *Curr Eye Res*. 2013;38:793–801.
22. Kwon S, Borrelli E, Fan W, Ebraheem A, Marion KM, Sadda SR. Repeatability of fluorescence lifetime imaging ophthalmoscopy in normal subjects with mydriasis. *Transl Vis Sci Technol*. 2019;8:15.
23. Gakamsky A, Duncan RR, Howarth NM, et al. Tryptophan and non-tryptophan fluorescence of the eye lens proteins provides diagnostics of cataract at the molecular level. *Sci Rep*. 2017;7:40375.
24. Weale RA. Human lenticular fluorescence and transmissivity, and their effects on vision. *Exp Eye Res*. 1985;41:457–473.
25. Sato K, Bando M, Nakajima A. Fluorescence in human lens. *Exp Eye Res*. 1973;16:167–172.
26. Sparrow JM, Neil HA, Bron AJ. Biometry and auto-fluorescence of the anterior ocular segment in diabetics with and without autonomic neuropathy: a case control study. *Eye (Lond)*. 1992;6:50–54.
27. Bessems GJ, Keizer E, Wollensak J, Hoenders HJ. Non-tryptophan fluorescence of crystallins from normal and cataractous human lenses. *Invest Ophthalmol Vis Sci*. 1987;28:1157–1163.
28. Van Heyningen R. Fluorescent glucoside in the human lens. *Nature*. 1971;230:393–394.
29. Truscott RJ, Wood AM, Carver JA, et al. A new UV-filter compound in human lenses. *FEBS Lett*. 1994;348:173–176.

30. Bron AJ, Vrensen GF, Koretz J, Maraini G, Harding JJ. The ageing lens. *Ophthalmologica*. 2000;214:86–104.
31. Klemm M, Schweitzer D, Peters S, Sauer L, Hammer M, Haueisen J. FLIMX: a software package to determine and analyze the fluorescence lifetime in time-resolved fluorescence data from the human eye. *PLoS One*. 2015;10:e0131640.
32. Schweitzer D, Hammer M, Schweitzer F, et al. In vivo measurement of time-resolved autofluorescence at the human fundus. *J Biomed Opt*. 2004;9:1214–1222.
33. Becker B, Bergmann A, Sauer L. Shifted-component model improves FLIO data analysis. Available at: https://www.becker-hickl.com/literature/application-notes/shifted-component-model-improves-flio-data-analysis/. Accessed June 26, 2020.
34. Klemm M, Blum J, Link D, Hammer M, Haueisen J, Schweitzer D. Combination of confocal principle and aperture stop separation improves suppression of crystalline lens fluorescence in an eye model. *Biomed Opt Express*. 2016;7:3198–3210.